© Indian Academy of Sciences

REGULAR ARTICLE

Nickel(II), copper(II) and zinc(II) complexes with an N-pendent dimethyl derivative of an octamethyl macrocyclic ligand: synthesis, characterization and antimicrobial studies

SUMAN KANTI DAS GUPTA[a], SASWATA RABI[a,b], DEPONKOR GHOSH[a],
FARHANA YASMIN[a], BENU KUMAR DEY[a], SUJAN DEY[c] and TAPASHI GHOSH ROY[a,*] [ORCID]

[a]Department of Chemistry, University of Chittagong, Chattogram 4331, Bangladesh
[b]Department of Chemistry, Chittagong University of Engineering & Technology, Chattogram 4349, Bangladesh
[c]Department of Microbiology, University of Chittagong, Chattogram 4331, Bangladesh
E-mail: tapashir57@gmail.com

Abstract. Interaction of CH_3I with L (3,10-C-meso-Me_8[14]diene) in the ratio of 4:1 in ethanolic solution at room temperature yielded N-pendent dimethyl derivative [(L-2H)(–CH_3)$_2$] denoted by L_Z. Interaction of nickel(II) acetate tetrahydrate with L_Z and subsequent addition of $NaClO_4 \cdot 6H_2O$ produced square planar orange-yellow product, [NiL_Z](ClO$_4$)$_2$. The reaction of copper(II) perchlorate hexahydrate with L_Z afforded four coordinated square planar red [CuL_Z](ClO$_4$)$_2$. However, on the reaction of zinc(II) nitrate hexahydrate with L_Z furnished white six coordinated two distereoisomeric complexes [Zn$L_{Z\alpha}$(NO$_3$)$_2$] and [Zn$L_{Z\beta}$(NO$_3$)$_2$]. Axial addition reactions on four coordinated square planar [NiL_Z](ClO$_4$)$_2$ with KX (X= SCN, NO$_3$, Cl, Br or I) and NaNO$_2$ resulted in six coordinated octahedral and square pyramidal axial addition products, such as [NiL_Z(NCS)$_2$], [NiL_Z(NO$_3$)(ClO$_4$)], [NiL_ZCl(ClO$_4$)], [NiL_ZBr$_2$], [NiL_ZI$_2$] and [NiL_Z(NO$_2$)](ClO$_4$), respectively. However axial substitution reactions on [Zn$L_{Z\alpha}$(NO$_3$)$_2$] with KY (Y= SCN, Cl or Br) and NaNO$_2$ produced six coordinated octahedral axial substitution products [Zn$L_{Z\alpha}$(NCS)$_2$], [Zn$L_{Z\alpha}$Cl$_2$], [Zn$L_{Z\alpha}$Br$_2$] and [Zn$L_{Z\alpha}$(NO$_2$)$_2$]. Similarly, the axial substitution reactions on [Zn$L_{Z\beta}$(NO$_3$)$_2$] with KI and $NaClO_4 \cdot 6H_2O$ resulted in six coordinated octahedral axial substitution products [Zn$L_{Z\beta}$I$_2$] and [Zn$L_{Z\beta}$(H$_2$O)$_2$](ClO$_4$)$_2$, respectively. The compounds have been characterized by analytical, spectroscopic, magnetochemical and conductivity data. The antimicrobial activities of the new ligand and its complexes have been tested against different micro pathogens.

Keywords. N-pendent dimethyl derivative; Copper(II); nickel(II) and zinc(II) complexes; Spectroscopic studies; Addition and substitution reactions; Antimicrobial studies.

1. Introduction

The area of macrocyclic chemistry is getting top priority to the scientists because of their fascinating criteria and notable applications in different sectors. Macrocyclic compounds are dominating remarkably in the region of medicinal chemistry by their excellent pharmacological activities.[1–9] Beside this, macrocyclic ligands and their various metal complexes are playing an important role in industrial,[10] analytical[11] and engineering sector also. However, the N-pendent derivatives of macrocycles and their complexes are also taking a good position in the research because of their multifarious applications. Reports on synthesis of different N-pendent macrocyclic ligands and their metal complexes by using different alkylating agents are noted in literatue.[12–16] Reports on metal complexes of fourteen membered octamethyl macrocyclic diene ligand (Me$_8$[14]diene),[17] isomeric ligands (L$_A$, L$_B$ & L$_C$)[18–20] are available in literature. Moreover, investigations on some N-pendent macrocyclic compounds and their complexes such as copper(II) and nickel(II)

complexes with bis-hydroxyethyl (L_{BY} and L_{CY}), dimethyl (L_{BZ}, L_{CZ}) derivatives of the isomeric ligands L_B and L_C are also described in our earlier reports.[12–14] Further cadmium(II) complexes of an N-pendent ligand L_{BX} (cyano ethyl derivative of L_B) were established successfully[15] with its X-ray crystallographic analysis.[16] But N-pendent derivative of the free diene ligand (Me_8[14]diene) (L) and its metal complexes have not been reported yet. So, it was reasonable to look over whether N-pendent derivative of free diene ligand and its metal complexes can be afforded or not. In this connection, N-pendent dimethyl derivative ligand L_Z of L was successfully prepared by (Scheme 1) using methyl iodide (CH_3I) as alkylating agents. Additionally, nickel(II), copper(II) and zinc(II) complexes with different orientation of L_Z were prepared not only by the direct reactions with metal salts but also by the axial substitution and addition reactions. So in this research work, we have reported the synthesis, characterization and antimicrobial activities of a new N-pendent dimethyl

derivative ligand L_Z and its nickel(II), copper(II) and zinc(II) complexes.

2. Experimental

2.1 *Material and equipment*

All chemicals were of analytical grade (Sigma Aldrich) or equivalent grade and were used without further purification. The solvents were of reagent grade. Equipment used were of standard ones. Such as Microanalyses of C, H, N and S of ligands and complexes have been carried out on Leco CHNS-932 elemental analyzer (LECO Corporation, St. Joseph, MI) at CARS, Dhaka University, Bangladesh. Melting points of the ligands as well as of the complexes were obtained with an electrothermal melting point apparatus at the Inorganic Research Laboratory of Chittagong University. The infrared spectra of the compounds were taken as KBr discs in the range 4000-400 cm^{-1} on a Shimadzu IR 20 spectrophotometer (Shimadzu, Kyoto, Japan) at the Department of Chemistry, University of Chittagong,
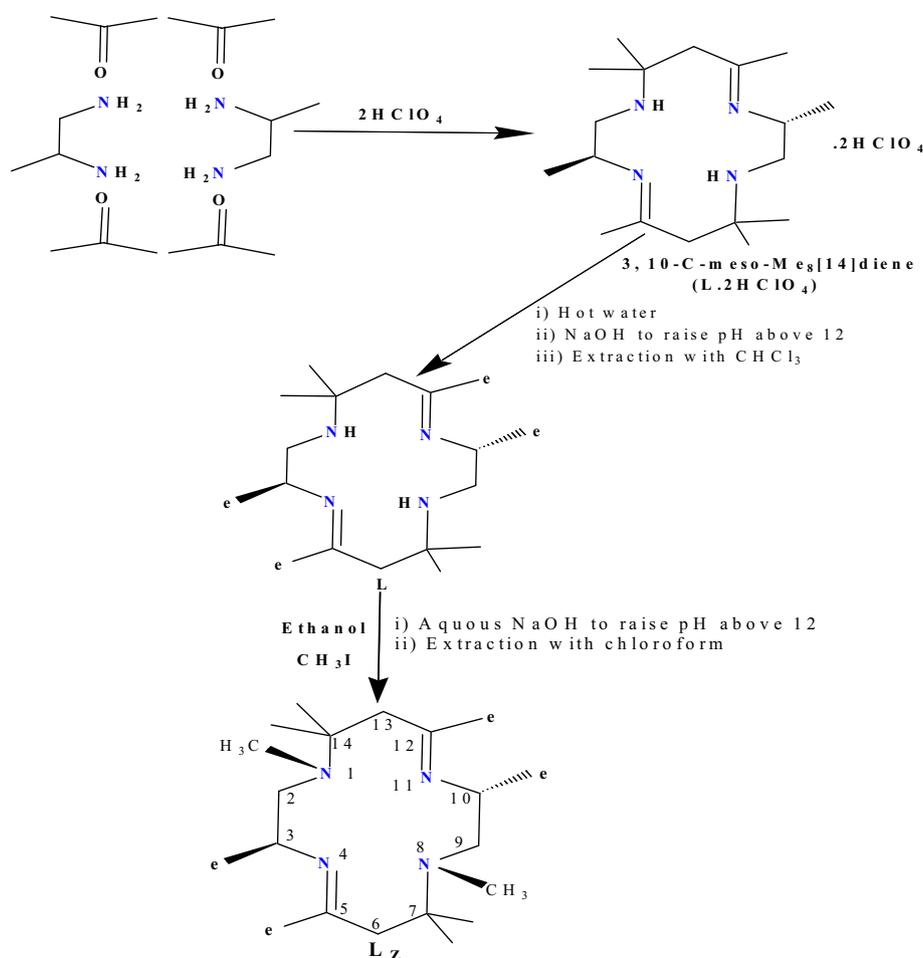
Scheme 1. Synthesis of N-pendent dimethyl ligand, L_Z.

Bangladesh. Conductance measurements of the complexes were done on a conductivity bridge HI-8820 (Hanna Instruments, Padova, Italy) in DMSO, H_2O and $CHCl_3$ solutions at the University of Chittagong. Electronic spectra of the samples were recorded on a UV-visible spectrophotometer (Shimadzu, Kyoto, Japan) at the Department of Chemistry, University of Chittagong, Bangladesh. The mass spectral measurements of the ligands were carried out at the Department of Chemistry, Friedrich Schiller University, Jena, Germany on a MAT 95XL Finnigan instrument (ThermoQuest Finnigan, Bremen, Germany) for electrospray ionization (ESI). ^{1}H-NMR and ^{13}C-NMR spectra of the samples were recorded on 400 MHz Bruker Gemini instrument at the Wazed Miah Science Research Centre (WMSRC), Jahangirnagar University, Bangladesh and Friedrich Schiller University, Jena, Germany on a Bruker AVANCE 400 spectrometer (Bruker AG, Karlsruhe, Germany). All the magnetic measurements have been carried out by SHERWOOD SCIENTIFIC magnetic susceptibility balance at the Department of Chemistry, University of Chittagong, Bangladesh which was calibrated using $Hg[Co(NCS)_4]$.

Precaution: Perchlorates are explosive at high temperature.

2.2 Synthesis of Ligands

2.2.1 Ligand salt L.2HClO$_4$ and free ligand L

The parent ligand salt $Me_8[14]$diene.$2HClO_4$ (3, 10-C-meso-L.$2HClO_4$) was prepared by the method described in literature[17,21] (Scheme 1). Then 20 g of 3,10-C-meso-$Me_8[14]$diene.$2HClO_4$ were suspended in 100 mL of water. To this, solid sodium hydroxide was added to raise the pH of the mixture above 12. Excess sodium hydroxide was added to the mixture to ensure that the ligand is free from hydroperchlorate. The mixture was heated on a water bath for half an hour. The free ligand was extracted several times with chloroform from the hot-mixture. The chloroform was then evaporated off living behind a yellow oily liquid. On cooling, the oily liquid was solidified to a white product, $Me_8[14]$diene [L].

2.2.2 N-pendent dimethyl derivative ligand, L$_Z$:

0.308 g (1.0 mmol) of L and 0.568 g (4.0 mmol) of methyl iodide were dissolved separately in 25 mL of dry ethanol and mixed. The reaction mixture was stirred for 12 h on a magnetic stirrer at room temperature. During this period white precipitate was formed, which was separated by filtration followed by washing with dry ethanol. Then the white solid was suspended in 20 mL aqueous NaOH solution to raise pH above 12. The mixture was extracted with chloroform, which on evaporation yielded white solid. This product was washed with diethylether and recrystallized from methanol and chloroform mixture, finally dried over silica gel in a vacuum desiccator and labelled as L$_Z$.

For L$_Z$ ($C_{20}H_{40}N_4$): Color: white. Melting Point: 90 °C Anal: Found: C, 71.32; H, 12.02; N, 16.61% Calc.: C,

71.37; H, 11.98; N, 16.65%. IR (cm^{-1}): ν_{C-C}, 1148w, ν_{C-H} 2952w, $\nu_{C=N}$ 1663s, ν_{CH3} 1378m, ν_{N-CH3} 2870s. Mass spectrum (Figure S2 and Table S1, Supplementary Information): Molecular ion peak, 336; Base peak 98; Fragment peaks, 308, 155, 139, 124, 98, 85, 70, 41.^{1}H NMR (δ, ppm in $CDCl_3$) (Figure S2, Supplementary Information): For CH_3 (geminal dimethyl), δ=1.037 (s, e, 6H), 1.194 (s, a, 6H); For methyl protons on sp^2 carbon, $\delta = 1.799$ (s, e, 6H); for CH_3 (Methyl on chiral carbon), $\delta = 0.936$ (d, e, 6H); for CH_2 & CH $\delta = 1.13$(m), 1.96(m), 2.29(m); for N-methyl protons, $\delta = 1.996$ (s, 3H), 2.132 (s, 3H). ^{13}C NMR (δ ppm in DMSO-d_6) (Figure S3, Supplementary Information): peripheral carbons, $\delta = 19.080, 19.664, 22.451, 24.251, 24.337, 27.645, 28.194, 30.723$; Ring carbons other than sp^2 carbons, $\delta = 32.376, 33.384, 46.281, 47.832, 48.667, 49.301, 50.044, 52.643$; Other carbons (N-$CH_3$) $\delta = 58.781, 60.454$, sp^2 carbons, $\delta = 167.910, 171.732$.

2.3 Metal complexes of L$_Z$

2.3.1 Nickel(II) complexes of L$_Z$

2.3.1.1 Nickel(II) complex [NiL$_Z$](ClO$_4$)$_2$:

0.337 g (1.0 mmol) of L$_Z$ and 0.249 g (1.0 mmol) of nickel(II) acetate tetrahydrate were dissolved separately in 50 mL cold and dry methanol. The ligand L$_Z$ solution was added dropwise to the boiling nickel(II) acetate solution with stirring. The reaction mixture was heated on a steam bath for 1h and the volume reduced to 20 mL while an orange color developed. After adding 0.5 g of sodium perchlorate hexahydrate, the solution was again heated for 10 min and allowed to stand for about 2 h. The orange-yellow product [NiL$_Z$](ClO$_4$)$_2$ was filtered off, washed with methanol followed by diethyl ether and dried under vacuum.

For [NiL$_Z$](ClO$_4$)$_2$ ($C_{20}H_{40}N_4Cl_2O_8Ni$): Color: Orange-Yellow. Decomposition point: 248 °C, Anal. Found: C, 40.42; H 6.83; N, 9.43%, Calc.: C, 40.43; H, 6.79; N, 9.43%. IR (cm^{-1}): ν_{C-H} 2989m, ν_{CH3} 1380m, ν_{C-C} 1147vw, $\nu_{C=N}$ 1670, ν_{ClO4} 624s, 1072vs, ν_{N-CH3} 2879. Molar conductivity ($ohm^{-1}cm^2mol^{-1}$) in DMSO, 84; in water, 204. Magnetic moment μ_{eff} (BM): Diamagnetic. UV vis [λ_{max} in nm (ε_{max})]: in DMSO, 439 (125), 589(16), 615 (25); in Water, 469(132), 384(1372). ^{1}H-NMR (δ, ppm in DMSO-d_6) (Fig.-S4): For CH_3 (gem dimethyl), δ =1.135 (s, e, 6H), 1.602 (s, a, 6H); for methyl protons on sp^2 carbon, δ= 2.231 (s, e, 6H); for methyl protons on chiral carbon, $\delta = 1.283$ (d, e, 6H); For CH_2 and CH, δ=2.781(m), 3.990 (m), 4.773 (m); for N-methyl protons, $\delta = 2.196$ (s, 6H).

2.3.1.2 Axial addition products of [NiL$_Z$](ClO$_4$)$_2$

2.3.1.2.1 [NiL$_Z$(NCS)$_2$]:

0.594 g (1.0 mmol) of [NiL$_Z$](ClO$_4$)$_2$ was suspended in 30 mL absolute methanol and 0.194 g (2.0 mmol) of KSCN was dissolved in 30 mL of the same solvent, then mixed together. A yellow color developed immediately. The reaction mixture was heated for 45 min and a white precipitate was removed by filtration.

Then the filtrate was dried by heating on a water bath and the residue was extracted with chloroform. The pink chloroform extract on drying gave yellow solid product $[NiL_Z(NCS)_2]$ which was stored in a vacuum desiccator over silica gel.

For $[NiL_Z(NCS)_2]$ $(C_{22}H_{40}N_6S_2Ni)$: Color: yellow. Decomposition point: 218 °C. Anal. Found: C, 51.67; H, 7.92; N, 16.40%, Calc.: C, 51.67; H, 7.88; N, 16.43%. IR (cm^{-1}): ν_{C-H}, 2971s, ν_{CH3} 1386vs, ν_{C-C} 1166vs, $\nu_{C=N}$ 1634s, ν_{CN} 2036vs, ν_{CS} 841m, ν_{NCS} 480s, ν_{N-CH3} 2849m, ν_{Ni-N} 516s. Molar conductivity (Λ_o, ohm^{-1}cm^{2}mol^{-1}) in DMSO, 40; in water, 243, in CHCl$_3$ 0. Magnetic moment μ_{eff} (B.M) 1.63. UV vis[λ_{max} in nm (ε_{max})]: in DMSO, 587(14), 620(32); in CHCl$_3$, 288(905), 390(134), 385(108), 595(28), 668(23); in water, 284(3378), 436(63).

2.3.1.2.2 $[NiL_Z(NO_3)(ClO_4)]$, $[NiL_Z(NO_2)](ClO_4)$, $[NiL_Z-Cl(ClO_4)]$, $[NiL_ZBr_2]$ and $[NiL_ZI_2]$: The axial addition products, $[NiL_Z(NO_3)(ClO_4)]$, $[NiL_Z(NO_2)](ClO_4)$, $[NiL_Z-Cl(ClO_4)]$, $[NiL_ZBr_2]$ and $[NiL_ZI_2]$ were prepared by the reactions of $[NiL_Z](ClO_4)_2$ with KNO$_3$, NaNO$_2$, KCl, KBr and KI, respectively by following the above procedure adopted for the preparation of $[NiL_Z(NCS)_2]$.

For $[NiL_Z(NO_3)(ClO_4)]$ $(C_{20}H_{40}N_5O_7Cl_2Ni)$: Decomposition point: 234 °C. Color: Pale yellow. Anal. Found: C, 40.52; H 6.85; N, 11.79%, Calc.: C, 40.57; H, 6.80; N, 11.83%. IR (cm^{-1}): ν_{C-H}, 2918 m, ν_{CH3} 1383vs, ν_{C-C} 1148 m, $\nu_{C=N}$ 1644s, ν_{NO3} 1451w, 1334s, ν_{ClO4} 624s, 1087m, ν_{N-CH3} 2849 m, ν_{Ni-N} 548m. Molar conductivity (Λ_o, ohm^{-1}cm^{2}mol^{-1}) in DMSO, 38, in water, 234, in CHCl$_3$ 0. Magnetic moment μ_{eff} (B.M): 1.53. UV vis [λ_{max} in nm (ε_{max})]: in DMSO, 563(15), 620(212); in CHCl$_3$, 600(37), 389(225), 263(1923); in water, 436(85), 280(1254).

For $[NiL_Z(NO_2)](ClO_4)$ $(C_{20}H_{40}N_5O_6Cl_2Ni)$: Decomposition point: 244 °C. Color: Pale yellow. Anal. Found: C, 41.72; H 7.02; N, 12.12%, Calc.: C, 41.69; H, 6.99; N, 12.16%. IR (cm^{-1}): ν_{C-H}, 2978w, ν_{CH3} 1377w, ν_{C-C} 1134w, $\nu_{C=N}$ 1637s, $\nu_{NO2(asym)}$ 1453w, $\nu_{NO2(sym)}$ 1377m, δ_{NO2} 841, ν_{ClO4} 624s, 1092s, ν_{N-CH3} 2878m, ν_{Ni-N}, 535s. Molar conductivity (Λ_o, ohm^{-1}cm^{2}mol^{-1}): in DMSO, 78 in water, 245. Magnetic moment μ_{eff}(B.M). 1.63. UV vis[λ_{max} in nm (ε_{max})]: in DMSO, 260(1923), 517(25), 725(7); in water, 463 (96), 490 (58), 285(2625).

For $[NiL_ZCl(ClO_4)]$ $(C_{20}H_{40}N_4Cl_3O_4Ni)$: Decomposition point: 220 °C. Color: Pale yellow. Anal. Found: C, 41.50; H, 6.99; N, 12.04%, Calc.: C, 41.44; H, 6.96; N, 12.08%. IR (cm^{-1}): ν_{C-H}, 2963w, ν_{CH3} 1376s, ν_{C-C} 1151w, $\nu_{C=N}$ 1657s, ν_{ClO4} 624vs 1085m, ν_{N-CH3} 2849m, ν_{Ni-N}, 569m. Molar conductivity (Λ_o, ohm^{-1}cm^{2}mol^{-1}) in DMSO, 68; in CHCl$_3$, 0; in water, 224. Magnetic moment μ_{eff} (B.M): 1.57. UV vis [λ_{max} in nm (ε_{max})]: in DMSO, 536(26), 492(127), 469(125); in CHCl$_3$, 588(25), 545(44), 392(125), 610(19); in water, 436(93), 278(1220).

For $[NiL_ZBr_2]$ $(C_{20}H_{40}N_4Br_2Ni)$: Decomposition point: 230 °C. Color: Pale yellow. Anal. Found: C, 43.29; H, 7.31; N, 10.05%, Calc.: C, 43.28; H, 7.26; N, 10.09%. IR (cm^{-1}): ν_{C-H}, 2967w, ν_{CH3} 1379m, ν_{C-C} 1170s, $\nu_{C=N}$ 1636s, ν_{N-CH3}

2849s, ν_{Ni-N} 550m. Molar conductivity (Λ_o, ohm^{-1}cm^{2}mol^{-1}) in water, 218; in CHCl$_3$, 0. Magnetic moment μ_{eff}: 1.63. UV vis[λ_{max} in nm (ε_{max})]: in CHCl$_3$, 545(23), 615(36); in water, 438(134), 275(1200).

For $[NiL_ZI_2]$ $(C_{20}H_{40}N_4I_2Ni)$: Decomposition point: 198 °C. Color: Yellow. Anal. Found: C, 37.06; H, 6.23; N, 8.60%, Calc.: C, 37.01; H, 6.21; N, 8.63%. IR (cm^{-1}): ν_{C-H}, 2967w, ν_{CH3} 1377m, ν_{C-C} 1168s, $\nu_{C=N}$ 1642, ν_{N-CH3} 2872s, ν_{Ni-N} 582m. Molar conductivity (Λ_o, ohm^{-1}cm^{2}mol^{-1}) in DMSO, 72; in CHCl$_3$, 0; in water, 199. Magnetic moment μ_{eff} (B.M): 1.71. UV vis [λ_{max} in nm (ε_{max})]: in DMSO, 430(83), 582(32), 605 (46), 290(2562); in CHCl$_3$, 582(26), 625(10); in water, 438(123).

2.3.2 Copper(II) complex $[CuL_Z](ClO_4)_2$: 0.263 g (1.0 mmol) of copper(II) perchlorate hexahydrate and 0.336 g (1.0 mmol) of L$_Z$ were dissolved separately in 25 mL hot methanol and then mixed. The resulting red solution was heated on a water bath for 15 min. Then the reddish product was formed immediately. For the completion of the reaction, the mixture was heated for more five min with continuous stirring. After cooling at room temperature, the brick-red product was separated by filtration and washed with methanol followed by diethyl ether and finally stored in a vacuum desiccator.

For $[CuL_Z](ClO_4)_2$ $(C_{20}H_{40}N_4Cl_2O_8Cu)$: Decomposition point: 274 °C. Color: Brick-red. Anal. Found: C, 40.14; H, 6.77; N, 9.31%, Calc.: C, 40.10; H, 6.73; N, 9.35%. IR (cm^{-1}): ν_{C-H}, 2982s, ν_{CH3} 1374s, ν_{C-C} 1178m, $\nu_{C=N}$ 1667s, ν_{ClO4}^- 622vs, 1092vs, ν_{N-CH3} 2883, ν_{Cu-N} 541m. Molar conductivity (Λ_o, ohm^{-1}cm^{2}mol^{-1}) in DMSO, 77; in water, 186. Magnetic moment μ_{eff} (B.M): 1.87. UV vis[λ_{max} in nm (ε_{max})]: in DMSO, 380(1449), 542(35), 439(35); in CHCl$_3$, 566(199), 527(421), 395(1420).

2.3.3 Zinc(II) complexes of L$_Z$

2.3.3.1 Zinc(II) complexes $[ZnL_{Z\alpha}(NO_3)_2]$ and $[ZnL_{Z\beta}(NO_3)_2]$ prepared by the direct interaction of L$_Z$ with zinc(II) nitrate: 0.336 g (1.0 mmol) of L$_Z$ and 0.297 g (1.0 mmol) of zinc(II) nitrate hexahydrate were dissolved separately in 50 mL cold and dry methanol. The ligand L$_Z$ solution was added dropwise to the boiling zinc(II) nitrate hexahydrate solution with stirring. The reaction mixture was heated on a steam bath for one hour and the volume reduced to 20 mL. A white product of $[ZnL_{Z\alpha}(NO_3)_2]$ was filtered off, washed with methanol followed by diethyl ether and dried in a desiccator over silica gel. The filtrate was collected and then allowed to cool. After one hour the white product of $[ZnL_{Z\beta}(NO_3)_2]$ was filtered, washed with methanol followed by diethyl ether and dried in a desiccator over silica gel.

For $[ZnL_{Z\alpha}(NO_3)_2]$ $(C_{20}H_{40}N_6O_6Zn)$: Decomposition point: 194 °C. Color: White. Anal. Found: C, 45.70; H, 7.63; N, 15.94%, Calc.: C, 45.67; H, 7.67; N, 15.98%. IR (cm^{-1}): ν_{C-H}, 2971s, ν_{CH3} 1383m, ν_{C-C} 1182s, $\nu_{C=N}$ 1659, ν_{NO3} 1372w, 1490w, ν_{N-CH3} 2882, ν_{Zn-N} 570m. Molar conductivity (Λ_o, ohm^{-1}cm^{2}mol^{-1}) in DMSO, 35; in

CHCl$_3$, 0; in water, 218. ^{1}H-NMR (δ, ppm in DMSO-d$_6$) (Fig.-S5): For CH$_3$ (gem dimethyl), δ=1.338 (s, e, 6H),1.383 (s, a, 6H); for methyl protons on sp^2 carbon, δ= 2.123 (s,6H); for methyl on chiral carbon, δ = 1.585 (d, a, 6H); for CH$_2$ and CH and NH, δ = 2.194, 2.555, 3.018, 3.228, 4.096; for N-methyl protons, δ = 2.029 (s, 6H).

For [ZnL$_{Z\beta}$(NO$_3$)$_2$] (C$_{20}$H$_{40}$N$_6$O$_6$Zn): Decomposition point: 185 °C. Color: White. Anal. Found: C, 45.71; H, 7.69; N, 15.96%, Calc.: C, 45.67; H, 7.67; N, 15.98%. IR (cm^{-1}): ν_{C-H}, 2971w, ν_{CH3} 1383w, ν_{C-C} 1182m, $\nu_{C=N}$ 1660, ν_{NO3} 1371w, 1487w, ν_{N-CH3} 2890, ν_{Zn-N} 560 m. Molar conductivity (Λ_o, ohm^{-1}cm^{2}mol^{-1}) in DMSO, 25; in CHCl$_3$, 0; in water, 254. ^{1}H-NMR (δ, ppm in DMSO-d$_6$) (Figure S6, Supplementary Information): For CH$_3$ (gem dimethyl), δ=1.337 (s, e, 6H),1.640 (s, a, 6H); for methyl protons on sp^2 carbon, δ = 2.125 (s, 6H); For methyl on chiral carbon, δ = 1.383 (d, e, 3H), 1.574 (d, a, 3H); For CH$_2$ and CH δ = 2.502, 2.926, 3.254, 4.133. For N-methyl protons, δ= 2.025 (s, 3H), 2.189 (s, 3H).

2.3.3.2 Axial substitution products of [ZnL$^{'}$(NO$_3$)$_2$] (L$^{'}$ = L$_{Z\alpha}$ or L$_{Z\beta}$)

2.3.3.2.1 [ZnL$_{Z\alpha}$(NCS)$_2$]: 0.526 g (1.0 mmol) of [ZnL$_{Z\alpha}$ (NO$_3$)$_2$] was suspended in 30 mL absolute methanol and 0.194 g (2.0 mmol) of KSCN was dissolved in 30 mL of the same solvent, then mixed together. The reaction mixture was heated for 45 min and a white precipitate was removed by filtration. Then the filtrate was dried by heating on a water bath and the residue was extracted with chloroform. The colorless chloroform extract on drying afforded white solid product [ZnL$_{Z\alpha}$(NCS)$_2$] which was stored in a vacuum desiccator over silica gel.

For [ZnL$_{Z\alpha}$(NCS)$_2$] (C$_{20}$H$_{40}$N$_6$S$_2$Zn): Decomposition point: 158 °C. Color: White. Anal. Found: C, 51.01; H, 7.76; N, 16.19%, Calc.: C, 50.99; H, 7.78; N, 16.22%. IR (cm^{-1}): ν_{C-H}, 2970s, ν_{CH3} 1373s, ν_{C-C} 1169m, ν_{Zn-N} 550, ν_{N-CH3} 2881, $\nu_{C=N}$ 1665s, ν_{CN} 2042vs, ν_{CS} 850m, δ_{NCS}, 485w. Molar conductivity (Λ_o, ohm^{-1}cm^{2}mol^{-1}) in DMSO, 78; in CHCl$_3$ 0, in water, 195.

2.3.3.2.2 [ZnL$_{Z\alpha}$(NO$_2$)$_2$], [ZnL$_{Z\alpha}$Cl$_2$] & [ZnL$_{Z\alpha}$Br$_2$] and [ZnL$_{Z\beta}$I$_2$] & [ZnL$_{Z\beta}$(H$_2$O)$_2$](ClO$_4$)$_2$: The axial substitution products [ZnL$_{Z\alpha}$(NO$_2$)$_2$], [ZnL$_{Z\alpha}$Cl$_2$] and [ZnL$_{Z\alpha}$Br$_2$] were prepared by axial substitution reactions of [ZnL$_{Z\alpha}$(NO$_3$)$_2$] with NaNO$_2$ KCl and KBr, respectively as per the above procedure adopted for the preparation of [ZnL$_{Z\alpha}$(NCS)$_2$]. Similarly, axial substitution products [ZnL$_{Z\beta}$I$_2$] and [ZnL$_{Z\beta}$(H$_2$O)$_2$](ClO$_4$)$_2$ were prepared by the interaction of [ZnL$_{Z\beta}$(NO$_3$)$_2$] with KI and NaClO$_4$.6H$_2$O, respectively.

For [ZnL$_{Z\alpha}$(NO$_2$)$_2$] (C$_{20}$H$_{40}$N$_6$O$_4$Zn): Decomposition point: 178 °C. Color: White. Anal. Found: C, 48.65; H, 8.20; N, 16.98%, Calc.: C, 48.63; H, 8.16; N, 17.01%. IR (cm^{-1}): ν_{C-H}, 2970m, ν_{CH3} 1371w, ν_{C-C} 1182w, ν_{Zn-N} 542w, ν_{N-CH3} 2849, $\nu_{C=N}$ 1660s, ν_{asym}(NO$_2$) 1442m, ν_{sym}(NO$_2$) 1371w δ_{NO2}, 827. Molar conductivity (Λ_o, ohm^{-1}cm^{2}mol^{-1}) in DMSO, 30; in CHCl$_3$, 0; in water, 235. ^{1}H-NMR (δ, ppm in DMSO-d$_6$) (Figure S7,

Supplementary Information): For CH$_3$ (gem dimethyl), δ = 1.278 (s, e, 6H), 1.339 (s, a, 6H); For methyl protons on sp^2 carbon, δ= 2.125 (s, 6H); For N-methyl protons, δ = 2.033 (s, 6H); For methyl on chiral carbon, δ =1.403 (ovd, a, 6H); For CH$_2$ and CH, δ = 2.831, 2.921, 3.020, 3.33, 4.092, 4.204;

For [ZnL$_{Z\alpha}$Cl$_2$] (C$_{20}$H$_{40}$N$_4$Cl$_2$Zn): Decomposition point: 194 °C. Color: White. Anal. Found: C, 50.84; H, 8.55; N, 11.82%, Calc.: C, 50.80; H, 8.53; N, 11.85%. IR (cm^{-1}): ν_{C-H}, 2969m, ν_{CH3} 1383s, ν_{C-C} 1119m, ν_{Zn-N} 554w, ν_{N-CH3} 2898, $\nu_{C=N}$ 1664s. Molar conductivity (ohm^{-1}cm^{2}mol^{-1}) in DMSO, 68; in CHCl$_3$ 0; in water, 120.

For [ZnL$_{Z\alpha}$Br$_2$]: Decomposition point: 184 °C. Color: White. Anal. Found: C, 42.72; H, 7.14; N, 9.98%, Calc.: C, 42.76; H, 7.18; N, 9.97%. IR (cm^{-1}): ν_{C-H} 2973m, ν_{CH3} 1370m, ν_{C-C} 1173s, ν_{Zn-N} 555m, ν_{N-CH3} 2880, $\nu_{C=N}$ 1659s. Molar conductivity (Λ_o, ohm^{-1}cm^{2}mol^{-1}) in DMSO, 28; in CHCl$_3$, 0; in water, 256. ^{1}H-NMR (δ, ppm in DMSO-d$_6$) (Figure S8, Supplementary Information): For CH$_3$ (Gem methyl), δ = 1.351 (s, e, 6H), 1.432 (s, a, 6H); For methyl protons on sp^2 carbon, δ = 1.690 (s, 6H); For N-methyl protons, δ = 2.130 (s, 6H); For methyl on chiral carbon, δ = 1.526 (d, a, 6H); For CH$_2$ and CH, δ = 2.480, 2.848, 3.371, 4.120.

For [ZnL$_{Z\beta}$I$_2$] (C$_{20}$H$_{40}$N$_4$I$_2$Zn): Decomposition point: 188 °C. Color: White. Anal. Found: C, 36.68; H, 6.12; N, 8.53%, Calc.: C, 36.63; H, 6.15; N, 8.54%. IR (cm^{-1}): ν_{C-H}, 2971vs, ν_{CH3} 1373vs, ν_{C-C} 1179s, ν_{Zn-N} 505s, ν_{N-CH3} 2881, $\nu_{C=N}$ 1660s. Molar conductivity (Λ_o, ohm^{-1}cm^{2}mol^{-1}) in DMSO, 79; in CHCl$_3$, 0; in water, 261.

For [ZnL$_{Z\beta}$(H$_2$O)$_2$](ClO$_4$)$_2$ (C$_{20}$H$_{44}$N$_4$O$_{10}$ClZn): Decomposition point: 196 °C. Color: White. Anal. Found: C, 39.92; H, 7.38; N, 9.35%, Calc.: C, 39.94; H, 7.37; N, 9.32%. IR (cm^{-1}): ν_{C-H}, 2973s, ν_{CH3} 1373vs, ν_{C-C} 1177m, ν_{Zn-N} 561m, ν_{N-CH3} 2849, $\nu_{C=N}$ 1660s, ν_{OH} 3391m, ν_{MO} 450m ν_{ClO4} 624vs, 1080s. Molar conductivity (Λ_o, ohm^{-1}cm^{2}mol^{-1}) in water, 206.

2.4 Antibacterial activities

By applying the disk diffusion method the antibacterial studies of the ligand and its complexes were inspected against some human pathogenic gram-positive and gram-negative bacteria. Dried and sterilized filter paper disc (6 mm in diameter) and Petri dishes (100 mm in diameter) were used during the experiment. At first, sterilized molten cooled agar (approx. 15 mL) was poured into the Petri dishes and after the solidification of the agar, the test microorganisms were outspread homogeneously over the Petri dishes with the help of a sterilized glass rod. Then the sample discs (socking with 0.1% complex solution), the standard antibiotic discs and the control discs (0.1% DMSO) were placed gently in the agar plates pre-inoculated with test bacteria. These plates were allowed to keep at low temperature (4 °C) for 2-4 h for maximum diffusion. Then

the plates were sealed and incubated in an inverted position at 37 °C for 24 h. After incubation, the diameter of the zone of inhibition was observed and measured in mm which expressed the activity of the complexes. By subtracting the values of control (DMSO) the results for all concerned compounds have been measured.

2.5   Antifungal activities

The *in vitro* antifungal activities of the ligand and its complexes against selected phytopathogenic fungi was assessed by the poisoned food technique. Potato Dextros Agar (PDA) was used as a growth medium. Dimethyl-sulphoxide was used as the solvent to prepare solutions of the tested compounds. The solutions were then mixed with the sterilized PDA to maintain concentrations of the compounds of 0.01% (ca. 3μL). 20 mL of these solutions were each poured into a Petri dish. After the medium had solidified, a 5 mm mycelial disc of each fungus was placed in the center of each assay plate, along with a control. Linear growth of the fungus was measured in mm after five days of incubation at 25±2 °C.

3.   Results and Discussion

3.1   Ligands

3.1.1 *Ligand salt L.2HClO₄ and free ligand L*: Ligand salt Me_8[14]diene.2HClO₄ and free ligand L have been characterized as per literature.[17,21]

3.1.2 *N-pendent dimethyl derivative ligand L_Z*: Infra-red spectrum of L_Z exhibits $\nu_{C=N}$, ν_{C-H}, ν_{CH3} and ν_{C-C} bands at 1663 cm^{-1}, 2952 cm^{-1}, 1378 cm^{-1} and 1148 cm^{-1}, respectively. Usually, compounds containing (-N-CH₃) groups show a ν_{C-H} band[22] below 3000 cm^{-1}. This ligand also displays ν_{N-CH3} band at 2870 cm,$^{-1}$ which indicates that hydrogen atom bonded with the ring nitrogen has been substituted by the methyl (-CH₃) groups. The mass spectrum of L_Z (Figure S2 and Table S1, Supplementary Information) shows several peaks of which one at m/z 336 can be attributed to the molecular ion M$^+$. The peak at m/z value corresponding to 308 can be attributed to the simultaneous loss of two CH₃ radicals from two N-CH₃ groups and successive acceptance of two H radicals to form parent molecular ion peak (M$^+$) of the ligand L. The other various peaks at m/z values 155, 139, 124, 98, 85, 70 and 41 corresponding to different fragments are observed in the mass spectrum of the ligand. Different fragments of the compound are evidence in support of the structural formula of L_Z. The ^{1}H-NMR spectrum of the ligand shows two singlets at 1.037 ppm and 1.194 ppm

corresponding to six protons (6H) each, these can be assigned to an equatorial and axial component of gem-dimethyl groups. One doublet at 0.936 ppm corresponds to 6 protons. This doublet can be assigned to a pair of equivalent equatorial chiral methyl groups. Such an arrangement is possible if two methyls on chiral carbons are meso and occupies a diequatorial configuration. The spectrum further displays a singlet at 1.799 ppm corresponding to six protons (6H) which can be assigned to methyl protons on two sp^2 carbons. Further two singlets at 1.996 ppm and 2.132 ppm corresponding to three protons (3H) each indicate the presence of N-substituted two methyl (-CH₃) groups. Other methylene and methine protons appear as multiplets at 1.31 ppm, 1.964 ppm, 2.228 ppm. The appearance of two singlets for two N-methyl groups attributed to distortion in the structure. The ^{13}C-NMR spectrum of L_Z displays twenty peaks, which correspond to twenty non-equivalent carbon atoms, indicating no symmetry in the molecule, which is also supported by its ^{1}H-NMR spectrum where two N-methyl signals were observed in two different positions. Among the twenty peaks first eight in the range of 19-31 ppm can be assigned to the eight peripheral carbons. Other two signals at 32.376 ppm and 37.384 ppm are due to β- carbon (more shielded ring carbons compared to other ring carbons). Other six signals are for the six different ring carbons in the range of 45-55 ppm. The spectrum further exhibits two peaks at 167.190 ppm and 171.732 ppm due to two sp^2 carbons. Two N-H protons substituted methyl (-N-CH₃) carbons show two signals at 58.781 ppm and 60.454 ppm. Though due to the incorporation of two small methyl groups, the stereochemistry i.e., diequatorial orientation of chiral methyls of parent ligand L remains intact, but due to distortion as predicted by ^{1}H-NMR spectrum, 20 peaks are observed due to 20 non-equivalent carbons. Thus all these evidence are in favor of the structure of N-pendent ligand L_Z as presented in Scheme 1.

3.2   Metal complexes of L_Z

3.2.1 *Nickel(II) complexes of L_Z*

3.2.1.1 *[NiL$_Z$](ClO₄)₂*: Interaction between nickel(II) acetate tetrahydrate and N-pendent ligand L_Z with the subsequent addition of NaClO₄. 6H₂O produced a four coordinated square planar yellow-orange complex [NiL$_Z$](ClO₄)₂. The infrared spectrum of this complex displays ν_{C-C}, ν_{C-H}, $\nu_{C=N}$ and ν_{CH3} bands at 1147 cm^{-1}, 2989 cm^{-1}, 1670 cm^{-1} and 1380 cm^{-1}, respectively and ν_{ClO4} bands at 1072 cm^{-1} and 624 cm^{-1}. The position, as well as non-splitting of band[23] at 1072 cm^{-1},

supports the non-coordination of ClO_4^- ions in this complex. The appearance of a band at 2879 cm^{-1} can be accounted for N-CH$_3$ group. The conductance value 204 ohm^{-1}cm^{2}mol^{-1} of this complex in water (color remains intact in this solvent) indicate that this complex is 1:2 electrolyte i.e., two ClO_4^- ions are out of coordination sphere as expected. Again, the molar conductivity value of 84 ohm^{-1}cm^{2}mol^{-1} in DMSO solution of this complex corresponding to 1:1 electrolyte can be assigned for equilibrium between square planar and octahedral geometry as per expression 01.

$$[NiL_Z](ClO_4)_2 \overset{DMSO}{\rightleftharpoons} [NiL_Z(ClO_4)_2] \qquad (01)$$
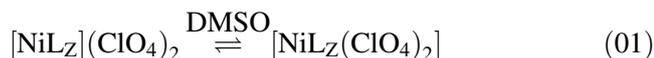
The magnetic moment value of the complex corresponding to diamagnetism is as expected for square planar orientation with dsp^2 hybridization. The electronic spectra of this complex display d-d bands at 434-469 nm in DMSO and water, which can be assigned for square planar nickel(II) complex. But the additional bands at 589-615 nm in DMSO corresponding to octahedral geometry[24] may be due to the equilibrium between square planar and octahedral geometry. The result of our studies, fit well with those of other macrocycles.[24] The higher value of ε_{max} in the visible region strongly support the existence of square planar configuration of this complex.[24] However, in the ultraviolet region, the absorption band at 384 nm is assignable to charge transfer transitions. The ^{1}H-NMR spectrum of this complex exhibits three sharp singlets at 1.135 ppm, 1.602 ppm and 2.231 ppm corresponding to 6H, 6H, and 6H, respectively. The singlets at 1.135 ppm and 1.602 ppm can be assigned to the gem dimethyl groups having equatorial and axial orientation, respectively. The third one at 2.231 ppm corresponding to 6H can be accounted for protons of methyl groups on sp^2 carbons at C$_5$ and C$_{12}$ positions. A singlet at 2.196 ppm was observed for N-methyl protons corresponding to 6H. The only doublet appearing at 1.283 ppm corresponding to 6H can be assigned to protons of methyl groups having equatorial orientation on chiral carbons. The other multiplets at 2.781 ppm,
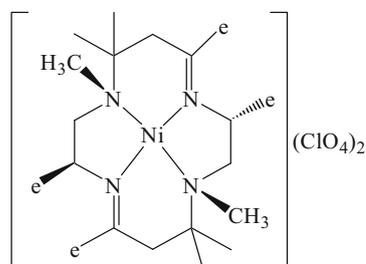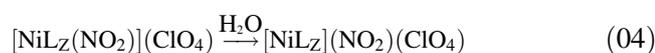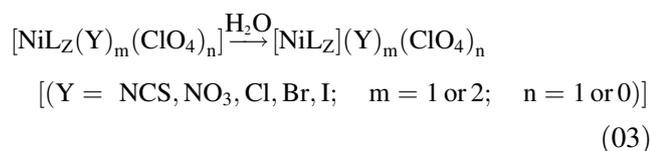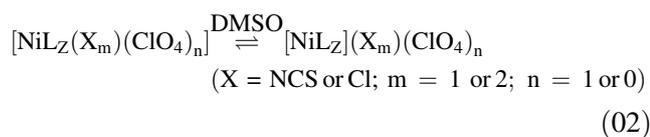

Str. 1. $[NiL_Z](ClO_4)_2$

3.990 ppm and 4.773 ppm can be attributed to the methine and methylene. So an all equatorial arrangement (Str. 1) of imine methyls on sp^2 carbon and methyls on chiral carbon can be assigned for this complex $[NiL_Z](ClO_4)_2$.

3.2.1.2 Axial addition products of $[NiL_Z](ClO_4)_2$

All the six coordinated octahedral axial addition reaction products $[NiL_Z(SCN)_2]$, $[NiL_Z(NO_3)(ClO_4)]$, $[NiL_Z(NO_2)](ClO_4)$, $[NiL_ZCl(ClO_4)]$, $[NiL_ZBr_2]$ and $[NiL_ZI_2]$ have been prepared by the interaction of four coordinated square planar $[NiL_Z](ClO_4)_2$ with KSCN, KNO$_3$, NaNO$_2$, KCl, KBr and KI, respectively. All the experimental data fit well with the molecular formula assigned. The infrared spectra of these complexes display ν_{C-C}, ν_{C-H}, $\nu_{C=N}$ and ν_{CH3} bands in the expected regions. Moreover, these complexes also reveal bands at 2849-2878 cm^{-1} and 516-582 cm^{-1} for ν_{N-CH3} and ν_{Ni-N}, respectively. Absence of ν_{ClO4} stretching bands at around 1080 & 625 cm^{-1} in $[NiL_Z(SCN)_2]$, $[NiL_ZBr_2]$, and $[NiL_ZI_2]$ can be accounted for substitution of ClO_4^- groups by the concerned anions and presence of ν_{CS}, ν_{CN} & δ_{NCS} band in $[NiL_Z(SCN)_2]$ can be safely assigned for substitution of ClO_4^- groups by NCS groups. Appearance of sharp ν_{CN} band at 2036 cm^{-1}, ν_{CS} band at 841 cm^{-1} and δ_{NCS} band at about 480 cm^{-1} of $[NiL_Z(SCN)_2]$ are therefore assigned for fully N-bonded thiocyanate group.[25–27] However, the spectra of $[NiL_Z(NO_3)(ClO_4)]$, $[NiL_Z(NO_2)](ClO_4)$ and $[NiL_ZCl(ClO_4)]$ display ν_{ClO4} bands at 1085-1092 cm^{-1} and 624 cm^{-1} indicating the presence of ClO_4^- in these complexes. However, the splitting of bands at around 1100 cm^{-1} of $[NiL_Z(NO_3)(ClO_4)]$ and $[NiL_ZCl(ClO_4)]$ can be accounted for a unidentate mode of coordination of ClO_4^-. But no splitting of that band in $[NiL_Z(NO_2)](ClO_4)$ attributes to ionic ClO_4^- group. Additionally, the spectrum of $[NiL_Z(NO_3)(ClO_4)]$ explores ν_{NO3} bands at 1451 cm^{-1} and 1334 cm^{-1} due to coordinated NO_3^- group but the separation of these bands by 117 cm^{-1} is attributed to the unidentate mode of coordination of NO_3^-.[24,27] Similarly the complex $[NiL_Z(NO_2)](ClO_4)$ exhibits the $\nu_{asym}(NO_2)$ and $\nu_{sym}(NO_2)$ bands at 1453 cm^{-1} and 1377 cm^{-1}, respectively and a band at 841 cm^{-1} due to δ_{NO2} frequency. However, since the IR spectra could not be run below 400 m^{-1} so ν_{Ni-Cl}, ν_{Ni-Br} and ν_{Ni-I} in halonickel(II) complexes could not be identified as they are expected around 260 cm^{-1}. The molar conductivity value 0 ohm^{-1}cm^{2}mol^{-1} for these complexes except $[NiL_Z(NO_2)](ClO_4)$ in CHCl$_3$ and 38-40 ohm^{-1}cm^{2}mol^{-1} for $[NiL_Z(NCS)_2]$ & $[NiL_Z(NO_3)(ClO_4)]$ in DMSO (colors remain intact in these solvents) supports the non-electrolytic nature of these complexes i.e., the anions are in the coordination sphere. But the molar conductivity values 50-72

ohm^{-1}cm^{2}mol^{-1} of the complexes [NiL$_Z$(SCN)$_2$] & [NiL$_Z$Cl(ClO$_4$)] in DMSO corresponding to 1:1 electrolyte[28] may be due to equilibrium between octahedral and square planar species as shown by the expression 02. However, the value of 78 ohm^{-1}cm^{2}mol^{-1} of [NiL$_Z$(-NO$_2$)](ClO$_4$) in the same solvent where the color of its solid sample remains intact is in accordance with formula assigned for its square pyramidal structure. Further molar conductivity values of 199-245 ohm^{-1}cm^2 mol^{-1} in water for these complexes indicate that these complexes are 1:2 electrolytes in this solvent indicating the conversion of octahedral/square pyramidal to square planar as presented by expression 03 & 04.

$$[NiL_Z(X_m)(ClO_4)_n] \overset{DMSO}{\rightleftharpoons} [NiL_Z](X_m)(ClO_4)_n$$
$$(X = NCS \text{ or } Cl; \ m = 1 \text{ or } 2; \ n = 1 \text{ or } 0)$$

(02)

$$[NiL_Z(Y)_m(ClO_4)_n] \overset{H_2O}{\longrightarrow} [NiL_Z](Y)_m(ClO_4)_n$$
$$[(Y = NCS, NO_3, Cl, Br, I; \quad m = 1 \text{ or } 2; \quad n = 1 \text{ or } 0)]$$

(03)

$$[NiL_Z(NO_2)](ClO_4) \overset{H_2O}{\longrightarrow} [NiL_Z](NO_2)(ClO_4)$$ (04)

The magnetic moment values of 1.53-1.71 BM of these octahedral nickel(II) complexes are indicative of paramagnetism of these complexes but less values compared to two unpaired electrons for sp^{3}d^2 hybridization can be accounted for partial conversion of octahedral to square planar spices in the air. The electronic spectra of these axial addition products except [NiL$_Z$(NO$_2$)](ClO$_4$), displays bands 385-392 nm, 545-595 nm and 600-668 nm for $^3A_{2g} \to {}^3T_{1g}(P)$, $^3A_{2g} \to {}^3T_{1g}(F)$ and $^3A_{2g} \to {}^3T_{2g}$ transition, respectively in CHCl$_3$ and DMSO which supports the six coordinated octahedral structure of theses complexes.[29–31] But the bands at 430-483 nm in DMSO for [NiL$_z$Cl(ClO$_4$)] & [NiL$_z$I$_2$] and 436-490 nm in water for all complexes comparatively in shorter wavelengths can be assigned to square planar species due to equilibrium between octahedral & square planar species and conversion of octahedral & square pyramidal to square planar, respectively. The molar conductivity values in DMSO also show the equilibrium between octahedral and square planar species. The lower extinction coefficient values also support the formation of octahedral complexes.[29–31] Electronic spectrum of [NiL$_Z$(NO$_2$)](ClO$_4$), reveals expected bands at 365-370 nm, 583-590 nm, 725-757 nm in concerned solvents assignable to the $^3B_{1g} \to {}^3E_g$ [T$_{1g}$(P)], $^1B_{2g} \to {}^1B_{1g}$, $^3B_{1g} \to {}^3B_{2g}$ [T$_{2g}$(F)] transitions, respectively which are characteristic bands expected for a high-

spin d^8 nickel(II) ion.[30,32] Though the ultraviolet region of this spectrum is not well-resolved, the absorption bands at 263-289 nm in all concerned solvents are assignable to charge transfer transition. Here the stereochemistry of the mother nickel(II) complex has been assigned by its ^{1}H-NMR spectral analysis and that of axial addition products on the basis that axial addition and substitution reactions take place without a change of conformation and configuration of the ligand of original complexes.[11,12,15,17] Based on all experimental and analytical data a common structure Str. 2a can be assigned for [NiL$_Z$(SCN)$_2$], [NiL$_Z$(NO$_3$)(ClO$_4$)], [NiL$_Z$Cl(ClO$_4$)], [NiL$_Z$Br$_2$] & [NiL$_Z$I$_2$] and Str. 2b for [NiL$_Z$(NO$_2$)](ClO$_4$).

3.2.2 Copper(II) complex, [CuL$_Z$](ClO$_4$)$_2$

Interaction between copper(II) perchlorate hexahydrate and N-pendent ligand L$_Z$ yielded a four coordinated square planar brick-red complex, [CuL$_Z$](ClO$_4$)$_2$. The infrared spectrum of this complex displays ν_{C-C}, ν_{C-H}, $\nu_{C=N}$ and ν_{CH3} bands in the expected regions. However it also exhibits ν_{ClO4} bands at 1092 cm^{-1} and 622 cm^{-1}, however, non-splitting of band at 1092 cm^{-1} supports the non-coordination of ClO$_4^-$ ions in [CuL$_Z$](ClO$_4$)$_2$. The appearance of an additional band at 2883 cm^{-1} can be accounted for N-CH$_3$ groups. The conductance value 186 ohm^{-1}cm^2 mol^{-1} of this complex in water indicates that this complex is 1:2 electrolyte i.e., two ClO$_4^-$ ions are out of coordination sphere as expected. The molar conductivity value of 77 ohm^{-1}cm^{2}mol^{-1}of the [CuL$_Z$](ClO$_4$)$_2$ in DMSO corresponding to 1:1 electrolyte can be assigned for an equilibrium (expression-05) between square planar and octahedral geometry as shown below.

$$[CuL_Z](ClO_4)_2 \overset{DMSO}{\rightleftharpoons} [CuL_Z(ClO_4)_2]$$ (05)
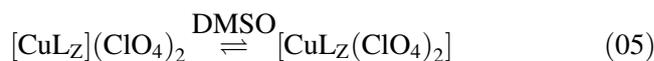
The magnetic moment value of the complex [CuL$_Z$](ClO$_4$)$_2$ is in good agreement with paramagnetic copper(II) complexes having one unpaired electron in their d^9 system. The electronic spectrum of this complex displays d-d band at 539-544 nm in DMSO and 527-566 nm in CHCl$_3$ due to $^2B_{1g} \to {}^2A_{1g}$ transition[33] and charge transfer bands at 380-395 nm in all concerned solvents.[34] Thus all experimental data support square planar structure. Since the ^{1}H-NMR spectrum of paramagnetic complexes is less informative, so the ^{1}H-NMR spectrum of this complex has not been measured. In this context, the stereochemistry i.e., axial-equatorial orientation has been assigned as corresponding square-planar nickel(II) complex. From the above discussion Str. 3 for [CuL$_Z$](ClO$_4$)$_2$ can be assigned.
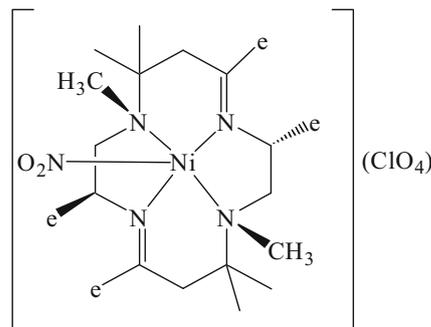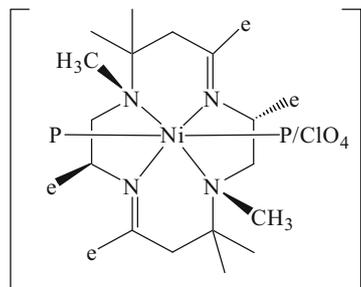
Str. 2. **a** [NiL$_Z$P$_x$(ClO$_4$)$_y$], (Where P = NCS, NO$_3$, Cl, Br or I; x = 1 or 2; y= 1 or 0), **b** [NiL$_Z$(NO$_2$)](ClO$_4$)
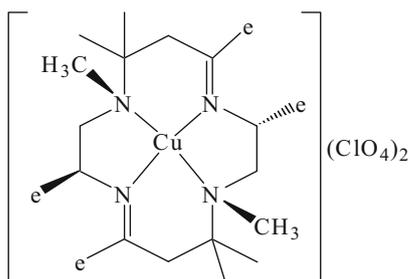
Str. 3. [CuL$_Z$](ClO$_4$)$_2$

3.2.3 *Zinc(II) complexes*

3.2.3.1 [ZnL$_{Z\alpha}$(NO$_3$)$_2$] & [ZnL$_{Z\beta}$(NO$_3$)$_2$]: Interaction of L$_Z$ with Zn(NO$_3$)$_2$.6H$_2$O furnished two diastereoisomeric complexes [ZnL$_{Z\alpha}$(NO$_3$)$_2$] and [ZnL$_{Z\beta}$(NO$_3$)$_2$]. The infrared spectra of these complexes exhibit ν_{CH3}, ν_{C-C}, $\nu_{C=N}$, ν_{C-H}, ν_{N-CH3} and ν_{Zn-N} bands in the expected regions. Additionally, the spectra further display bands at 1371-1372 cm^{-1} and 1487-1490 cm^{-1} for NO$_3^-$ and the separations of bands by 116-118 cm^{-1} are attributed to coordinated NO$_3^-$ groups.[23,27] The molar conductivity values of the complexes [ZnL$_{Z\alpha}$(NO$_3$)$_2$] and [ZnL$_{Z\beta}$(NO$_3$)$_2$] are 0 ohm^{-1}cm^2 mol^{-1} in CHCl$_3$ and 35 & 25 ohm^{-1}cm^{2}mol^{-1} in DMSO, respectively which indicate the non-electrolytic nature[28] of these complexes. But the values 218-254 ohm^{-1}cm^{2}mol^{-1} in water can be attributed for the formation of diaqua complexes as shown by expression 06.

$$[Zn(L')((NO_3)_2)] \xrightarrow[(L'=L_{Z\alpha} \text{ or } L_{Z\beta})]{\text{Water}} [ZnL'(H_2O)_2](NO_3)_2$$

(06)
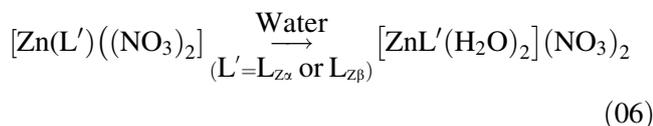
The ^{1}H-NMR spectrum of [ZnL$_{Z\alpha}$(NO$_3$)$_2$] explores four singlets at 1.338 ppm, 1.383 ppm, 2.029 ppm and 2.123 ppm corresponding to 6H each and are assigned to the equatorial components of gem-dimethyl protons, axial components of gem dimethyl protons, methyl protons on N atoms and methyl protons on sp^2 carbon atoms. The spectrum further shows one doublet at 1.585 ppm (6H) which can be assigned to two axial methyl groups on two chiral carbons. Hence, [ZnL$_{Z\alpha}$(NO$_3$)$_2$] is found to have two axially oriented methyl groups on two chiral carbons. The spectrum further displays multiplets at 2.194 ppm, 2.555 ppm, 3.018 ppm, 3.228 ppm, 4.096 ppm etc. due to CH$_2$ and CH protons. So a diaxial structure (Str. 4) can be assigned for [ZnL$_{Z\alpha}$(NO$_3$)$_2$]. The ^{1}H-NMR spectrum of the other diastereoisomer [ZnL$_{Z\beta}$(NO$_3$)$_2$] exhibits five singlets at 1.337 ppm, 1.640 ppm, 2.025 ppm, 2.125 ppm and 2.189 ppm corresponding to 6H, 6H, 3H, 6H and 3H, respectively. These singlets can be assigned to equatorial components of gem-dimethyls, axial components of gem-dimethyls, methyl protons on one chiral N- atom, methyl protons on sp^2 carbons and methyl protons on other chiral N-atom, respectively. The appearance of two doublets each due to 3H at 1.383 ppm and 1.574 ppm can be assigned to equatorial methyl on one chiral carbon and axial methyl on another chiral carbon, respectively. The spectrum further displays multiplets at 2.502 ppm, 2.926 ppm, 3.254 ppm, 4.133 ppm, etc., which can be due to CH$_2$ and CH protons. Thus an axial-equatorial orientation (Str. 5) has been assigned to this diastereoisomer, [ZnL$_{Z\beta}$(NO$_3$)$_2$].
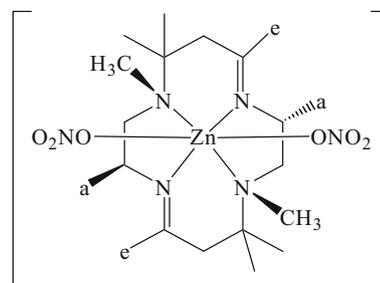
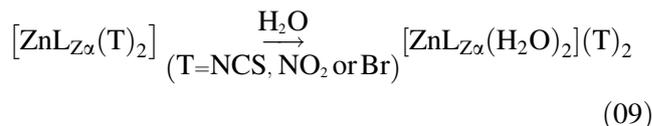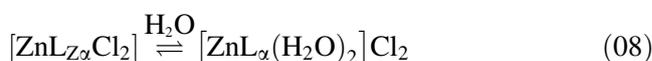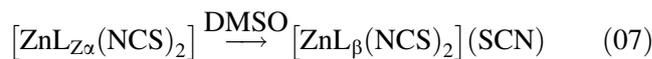**Str. 4.** [ZnL$_{Z\alpha}$(NO$_3$)$_2$]
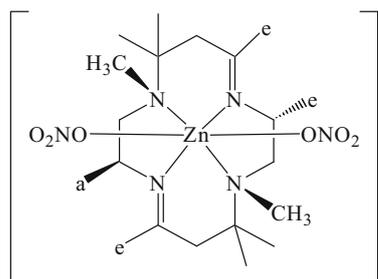
Str. 5. $[ZnL_{Z\beta}(NO_3)_2]$

### 3.2.3.2 Axial substitution products of $[ZnL'(NO_3)_2]$ ($L' = L_{Z\alpha}$ or $L_{Z\beta}$)

3.2.3.2.1 Axial substitution products of $[ZnL_{Z\alpha}(NO_3)_2]$

$[ZnL_{Z\alpha}(NO_3)_2]$ underwent axial substitution reactions with KSCN, NaNO$_2$, KCl and KBr to yield $[ZnL_{Z\alpha}(NCS)_2]$, $[ZnL_{Z\alpha}(NO_2)_2]$, $[ZnL_{Z\alpha}Cl_2]$ and $[ZnL_{Z\alpha}Br_2]$, respectively. Infrared spectra of these complexes exhibit ν_{CH3}, ν_{C-C}, $\nu_{C=N}$, ν_{C-H}, ν_{N-CH3} and ν_{Zn-N} bands in the expected regions. Absence of ν_{NO3} stretching bands demonstrate that the NO$_3^-$ groups are completely replaced by the concerned axial ligands. A sharp ν_{CN} band at 2042 cm^{-1}, ν_{CS} band at 850 cm^{-1} and δ_{NCS} band at about 485 cm^{-1} for $[ZnL_{Z\alpha}(NCS)_2]$ are assigned for fully N-bonded thiocyanate group.[25–27] Moreover, the complex $[ZnL_{Z\alpha}(NO_2)_2]$ exhibits the $\nu_{asym}(NO_2)$ and $\nu_{sym}(NO_2)$ bands at 1442 cm^{-1} and 1371 cm^{-1}, respectively. Bands at around 260 cm^{-1} for Zn-Cl and Zn-Br in $[ZnL_{Z\alpha}Cl_2]$ and $[ZnL_{Z\alpha}Br_2]$, respectively could not be detected because the spectra could not be measured below 400 cm^{-1}. The molar conductivity value of 0 ohm^{-1}cm^{2}mol^{-1} for these complexes in CHCl$_3$ and 18-30 ohm^{-1}cm^{2}mol^{-1} in DMSO except $[ZnL_{Z\alpha}(NCS)_2]$ support the non-electrolytic nature of them. But the value 78 ohm^{-1}cm^{2}mol^{-1} in DMSO for $[ZnL_{Z\alpha}(NCS)_2]$ and that of 68 ohm^{-1}cm^{2}mol^{-1} in water for $[ZnL_{Z\alpha}Cl_2]$ corresponding to 1:1 electrolyte may be due to conversion to square pyramidal species (expression-07) and equilibrium (expression-08) between octahedral dichloride and diaqua complexes, respectively. Again the values of 195-256 ohm^{-1}cm^{2}mol^{-1} in the water of $[ZnL_{Z\alpha}(NCS)_2]$, $[ZnL_{Z\alpha}(NO_2)_2]$ and $[ZnL_{Z\alpha}Br_2]$ indicate that these complexes are 1:2 electrolytes in this solvent which may be due to conversion of non-electrolyte to 1:2 electrolytes as expressed by the expression-09 where these complexes convert into diaqua complexes.
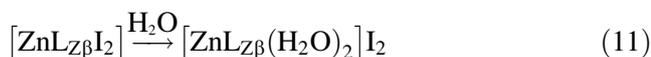
$$[ZnL_{Z\alpha}(NCS)_2] \xrightarrow{DMSO} [ZnL_\beta(NCS)_2](SCN) \qquad (07)$$

$$[ZnL_{Z\alpha}Cl_2] \xrightleftharpoons{H_2O} [ZnL_\alpha(H_2O)_2]Cl_2 \qquad (08)$$

$$[ZnL_{Z\alpha}(T)_2] \xrightarrow[(T=NCS,\ NO_2\ or\ Br)]{H_2O} [ZnL_{Z\alpha}(H_2O)_2](T)_2$$

$$(09)$$

The ^{1}H-NMR spectrum of $[ZnL_{Z\alpha}(NO_2)_2]$ exhibits four singlets at 1.278 ppm, 1.339 ppm, 2.033 ppm and 2.125 ppm each corresponding to six protons. These singlets can be assigned to equatorial components of gem-dimethyls, axial components of gem-dimethyls, methyls on N-atoms and methyls on sp^2 carbons, respectively. The spectrum also explores an overlapped doublet at 1.403 ppm corresponding to 6H assignable to two axially oriented methyl groups on two chiral carbons. So a diaxial arrangement of methyls on chiral carbons has been assigned as assigned for the mother complex. Similarly, the ^{1}H-NMR spectrum of $[ZnL_{Z\alpha}Br_2]$ also displays the same spectral pattern like $[ZnL_{Z\alpha}(NO_2)_2]$. Thus, diaxially oriented structure has been assigned to this complex too as assigned to its parent complex $[ZnL_{Z\alpha}(NO_3)_2]$. The diaxial orientation of these substituted products also again proves that axial substitution takes place without a change of conformation and configuration of the ligand of the original complex.[11,12,15,17] Based on these evidences a common Str. 6 can be assigned for $[ZnL_{Z\alpha}(NCS)_2]$, $[ZnL_{Z\alpha}(NO_2)_2]$, $[ZnL_{Z\alpha}Cl_2]$ and $[ZnL_{Z\alpha}Br_2]$.

3.2.3.2.2 Axial substitution products of $[ZnL_{Z\beta}(NO_3)_2]$:

$[ZnL_{Z\beta}I_2]$ and $[ZnL_{Z\beta}(H_2O)_2](ClO_4)_2$ were produced by the axial substitution reactions on $[ZnL_{Z\beta}(NO_3)_2]$ with KI and NaClO$_4$.6H$_2$O, respectively. Infrared spectra of these complexes were found to exhibit ν_{CH3}, ν_{C-C}, $\nu_{C=N}$, ν_{C-H}, ν_{N-CH3} and ν_{Zn-N} bands in the expected regions. The infrared spectrum of $[ZnL_{Z\beta}(H_2O)_2](ClO_4)_2$ further displays ν_{ClO4}^- bands
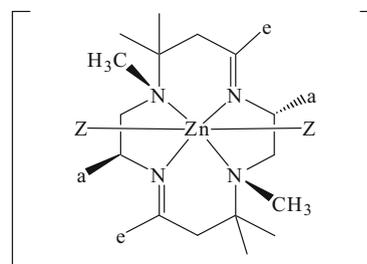
Str. 6. $[ZnL_{Z\alpha}Z_2]$ (Where Z =NCS, NO$_2$, Cl or Br)

at 1080 cm^{-1} and 624 cm^{-1} and no splitting of the band at 1080 cm^{-1} is an indication that the ClO_4^- is not in the coordinated state. Additionally, the spectrum reveals ν_{OH} at 3391 cm^{-1} and M-O band at 450 cm^{-1} which can be safely assigned for coordinated H_2O molecules.[22,27] The molar conductivity value 0 ohm^{-1}cm^2 mol^{-1} in CHCl$_3$ of [ZnL$_{Z\beta}$I$_2$] is in support of the non-electrolytic nature of this complex. However, conductivity value 79 ohm^{-1}cm^2 mol^{-1} in DMSO of the same corresponding to 1:1 electrolyte can be demonstrated by three ways as shown in expression-10(a-c), but the expressions 9(a) is more favorable as it involves no incorporation of any big molecule like DMSO. Again the value of 261 ohm^{-1}cm^2 mol^{-1} in water demonstrates that this complex is 1:2 electrolyte due to conversion as shown in expression 11. However, the value 206 ohm^{-1}cm^{2}mole^{-1} in the water of [ZnL$_{Z\beta}$(H$_2$O)$_2$](ClO$_4$)$_2$ corresponds to 1:2 electrolyte as expected. So, based on these facts, the following structure, Str. 7 can be assigned for the complexes [ZnL$_{Z\beta}$I] and [ZnL$_{Z\beta}$(H$_2$O)$_2$](ClO$_4$)$_2$.

$$\left[ZnL_{Z\beta}I_2\right] \xrightarrow{DMSO} \left[ZnL_{Z\beta}I\right]I \qquad (10a)$$

$$Or\left[ZnL_{Z\beta}I_2\right] \xrightarrow{DMSO} \left[ZnL_{Z\alpha}I(DMSO)\right]I \qquad (10b)$$

$$Or\left[ZnL_{Z\beta}I_2\right] \xrightleftharpoons{DMSO} \left[ZnL_{Z\beta}(DMSO)_2\right]I_2 \qquad (10c)$$

$$\left[ZnL_{Z\beta}I_2\right] \xrightarrow{H_2O} \left[ZnL_{Z\beta}(H_2O)_2\right]I_2 \qquad (11)$$
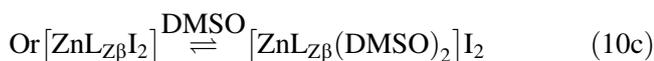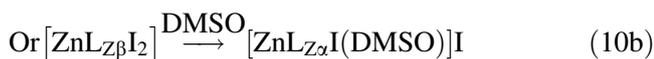
3.3 Antifungal activities

The in vitro evaluation results of antifungal activities of the concerned ligand, its metal complexes, noncoordinated metal salts and standard fungicide, Griseofulvin are shown in Table 6.4. From the results, it is evident
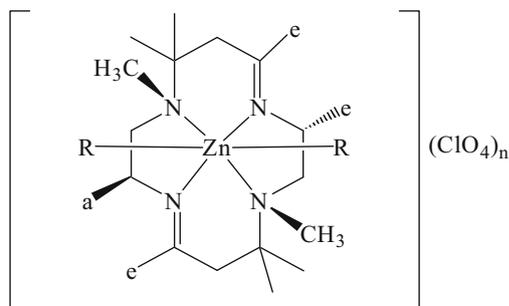
Str. 7. [ZnL$_{Z\beta}$R$_2$](ClO$_4$)$_n$ (Where R =I or H$_2$O; n=0 or 2)

that almost all complexes are sensitive towards all the used four fungal phytopathogens (Table 1). Some of these complexes are found to be more sensitive than standard Griseofulvin against all phytopathogens. Generally, most of the compounds show remarkable activities (100%) against all except *Fusarium equiseti* for which only [NiL$_Z$](ClO$_4$)$_2$ & [NiL$_Z$I$_2$] explored 100% potentiality. It was encouraging to notice that most of the test chemicals are very much sensitive towards the tested fungal phytopathogens which have not been observed in our previous studies. Though in our some previous studies[12,17,20] antifungal activities were found to decrease upon complexation most of these complexes exhibit higher potentiality than the ligand as our some other studies.[12,17,20]

3.4 Antibacterial activities

The synthetic macrocyclic ligands and their metal complexes showed activities of different grade against experimental pathogenic bacterial strains (Tables 2, 3). As per our earlier studies,[4,12,15,17] ligands did not show any activity against the bacteria and similar inactiveness also are shown by the present ligand against experimental bacteria. In this study, zinc(II) and copper(II) complexes are showing good activities than the nickel(II) complexes such as the zinc(II) complexes [ZnL$_{Z\alpha}$(NO$_3$)$_2$], [ZnL$_{Z\beta}$(NO$_3$)$_2$], [ZnL$_{Z\alpha}$(SCN)$_2$] and [ZnL$_{Z\alpha}$Cl$_2$] against *Bacillus cereus, Bacillus subtilis* & *Escherichia coli*; [ZnL$_{Z\beta}$I$_2$] & [ZnL$_{Z\beta}$(NO$_3$)$_2$] against *Bacillus subtilis* explore good potentiality. Whereas only copper(II) complex [CuL$_{AZ}$](ClO$_4$)$_2$ exhibit promising activity against all bacteria except *B. subtilis* & *K. pneumonia*. Similarly, the nickel(II) complexes [NiL$_Z$](ClO$_4$)$_2$ & [NiL$_Z$(NO$_2$)](ClO$_4$) showed good activities against *Bacillus cereus*. On the other hand, the mentionable activity was observed for the nickel(II) complex [NiL$_Z$(NO$_3$)(ClO$_4$)] against *Bacillus megatarium*. Antibacterial activity of concerned non-coordinated metal salt, solvent DMSO (as control) and standard medication, Ampicillin was also evaluated for the comparison. Though the ligand and the metal salts themselves are slightly poisonous, the stability of the complexes (very much stable even in solutions) prevents the liberation of ligands or metal ions in the test media.[3] However no definite trend can be derived from the observations at this stage but the positive results suggest further studies are warranted. In the case of disc diffusion methods, the zone of inhibition of the compounds is related to the susceptibility of the isolate and diffusion rate of drug through agar medium.[35] Chelation theory

Table 1. Inhibition of mycelial growth of the compounds.

	% Inhibition of mycelial growth			
Ligand and Complexes	*Rhizopus*	*Aspergillus niger*	*Fusarium equiseti*	*Aspergillus flavus*
L_Z	37	49	46	95
$[NiL_Z](ClO_4)_2$	43	46	100	43
$[NiL_Z(SCN)_2]$	100	100	49	100
$[NiL_ZCl(ClO_4)]$	58	100	95	100
$[NiL_ZBr_2]$	50	100	45	100
$[NiL_ZI_2]$	40	100	100	100
$[NiL_Z(NO_3)(ClO_4)]$	100	100	15	100
$[NiL_Z(NO_2)](ClO_4)$	100	100	15	100
$[CuL_Z](ClO_4)_2$	100	100	30	100
$[ZnL_{Z\alpha}(NO_3)_2]$	100	100	34	100
$[ZnL_{Z\beta}(NO_3)_2]$	100	42	50	100
$[ZnL_{Z\alpha}(SCN)_2]$	100	100	46	39
$[ZnL_{Z\alpha}(NO_2)_2]$	65	100	62	100
$[ZnL_{Z\alpha}Cl_2]$	63	100	47	100
$[ZnL_{Z\alpha}Br_2]$	72	100	42	100
$[ZnL_{Z\beta}I_2]$	36	100	56	100
$[ZnL_{Z\beta}(H_2O)_2](ClO_4)_2$	100	100	39	100
Griseofulvin (Standard)	45	46	20	39
$Ni(CH_3-COO)_2.4H_2O$	32	36	25	20
$CuCl_2$	75	66	23	55
$Zn(NO_3)_2$	14	0	0	11

Table 2. Antibacterial activities of the compounds against gram-positive bacteria.

	Diameter of the zone of inhibition in mm			
	Staphylococus aureus	*Bacillus cereus*	*Bacillus megaterium*	*Bacillus subtilis*
Ligand and complexes		48 hours incubation		
L_Z	0	0	0	0
$[NiL_Z](ClO_4)_2$	8	9	0	5
$[NiL_Z(SCN)_2]$	0	9	5	0
$[NiL_ZCl(ClO_4)]$	7	0	0	8
$[NiL_ZBr_2]$	6	0	8	0
$[NiL_ZI_2]$	0	6	0	0
$[NiL_Z(NO_3)(ClO_4)]$	0	0	11	8
$[NiL_Z(NO_2)](ClO_4)$	9	9	0	0
$[CuL_Z](ClO_4)_2$	11	14	10	0
$[ZnL_{Z\alpha}(NO_3)_2]$	5	9	11	17
$[ZnL_{Z\beta}(NO_3)_2]$	0	11	5	17
$[ZnL_{Z\alpha}(SCN)_2]$	0	13	0	15
$[ZnL_{Z\alpha}(NO_2)_2]$	0	0	0	7
$[ZnL_{Z\alpha}Cl_2]$	10	15	8	11
$[ZnL_{Z\alpha}Br_2]$	0	0	0	8
$[ZnL_{Z\beta}I_2]$	4	0	0	11
$[ZnL_{Z\beta}(H_2O)_2](ClO_4)_2$	0	0	0	8
Ampicillin (Standard)	24	25	29	27
$Ni(CH_3-COO)_2.4H_2O$	9	10	13	9
$CuCl_2$	20	14	15	16
$Zn(NO_3)_2$	8	9	10	8
Control	0	0	0	0

Table 3. Antibacterial activities of the compounds against gram-negative bacteria.

Ligand and Complexes	Diameter of zone of inhibition in mm			
	Salmonella typhi	*Pseudomonu saeruginosa*	*Escherichia coli*	*Klebsiella pneumoniae*
L_Z	0	0	0	0
$[NiL_Z](ClO_4)_2$	6	8	5	0
$[NiL_Z(SCN)_2]$	0	7	0	0
$[NiL_ZCl(ClO_4)]$	6	0	0	7
$[NiL_ZBr_2]$	0	0	0	7
$[NiL_ZI_2]$	5	0	7	0
$[NiL_Z(NO_3)(ClO_4)]$	0	0	0	5
$[NiL_Z(NO_2)](ClO_4)$	0	0	0	0
$[CuL_Z](ClO_4)_2$	11	8	7	0
$[ZnL_{Z\alpha}(NO_3)_2]$	0	0	10	0
$[ZnL_{Z\beta}(NO_3)_2]$	0	7	11	11
$[ZnL_{Z\alpha}(SCN)_2]$	0	0	13	0
$[ZnL_{Z\alpha}(NO_2)_2]$	0	0	0	0
$[ZnL_{Z\alpha}Cl_2]$	0	0	15	11
$[ZnL_{Z\alpha}Br_2]$	6	0	0	0
$[ZnL_{Z\beta}I_2]$	0	0	0	10
$[ZnL_{Z\beta}(H_2O)_2](ClO_4)_2$	0	0	0	0
Ampicillin (Standard)	22	34	26	25
$Ni(CH_3\text{-}COO)_2.4H_2O$	12	11	11	11
$CuCl_2$	16	14	12	13
$Zn(NO_3)_2$	13	12	12	12
Control	0	0	0	0

can explain the mechanism of antibacterial activities[36] i.e increase of activity due to chelation. Additionally, it can be stated that blockage of the synthesis of protein can restricts further growth of the organism.[37]

4. Conclusions

Condensation of acetone with 1,2-diamino propane in presence of the quantitative amount of $HClO_4$ produced $Me_8[14]$diene.$2HClO_4$ (L.$2HClO_4$) which on extraction with chloroform at pH above 12 yielded free diene ligand $Me_8[14]$diene (L). L on interaction with methyl iodide (CH_3I) afforded an N-dimethyl derivative L_Z where two methyl (-CH_3) groups are on two N-atoms of L. The concerned N-methyl derivative ligand L_Z underwent facile complexation when reacted with nickel(II) acetate by subsequent addition of $NaClO_4.6H_2O$ and copper perchlorate hexahydrate to produce square planar complexes $[NiL_Z](ClO_4)_2$ and $[CuL_Z](ClO_4)_2$, respectively. Further, $[NiL_Z](ClO_4)_2$ underwent axial addition reactions with SCN^-, NO_3^-, NO_2^-, Cl^-, Br^- and I^- and $NaClO_4.6H_2O$ to produce corresponding addition products. However, this N-pendant dimethyl derivative ligand, L_Z furnished six coordinated diastereoisomeric octahedral complexes

$[ZnL_{Z\alpha}(NO_3)_2]$ & $[ZnL_{Z\beta}(NO_3)_2]$ when reacted with zinc(II) nitrate hexahydrate. The diastereoisomers $[ZnL_{Z\alpha}(NO_3)_2]$ and $[ZnL_{Z\beta}(NO_3)_2]$ underwent axial substitution reactions with SCN^-, NO_2^-, Cl^-, Br^-, I^- and $NaClO_4.H_2O$ to yield six coordinated octahedral axial substitution products. The compounds showed excellent antifungal activities but did not reveal very promising antibacterial activities.

Supplementary Information (SI)

The synthesis of N-pendent ligand L_Z has been shown in Scheme S1 (Supplementary Information). IR spectra, mass spectra & fragmentation pattern, ^{1}H-NMR and ^{13}C-NMR spectra for the newly synthesized N-pendent ligand L_Z have been included in, Figure-S1, Figure S2 & Table S1, Figure S3 and Figure S4, respectively. However, some representative IR spectra

of metal complexes of L_Z have been shown in Figure S5 to Figure S11. On the other hand ^{1}H-NMR spectra for $[NiL_Z](ClO_4)_2$, $[ZnL_{Z\alpha}(NO_3)_2]$, $[ZnL_{Z\beta}(-NO_3)_2]$, $[ZnL_{Z\alpha}(NO_2)_2]$ and $[ZnL_{Z\alpha}Br_2]$ have been added as Figure S12, Figure S13, Figure S14, Figure S15 and Figure S16, respectively. Some UV spectra of Ni(II) and Cu(II) complexes of N-pendent ligand L_Z have been included in Figure S17. The nickel(II), copper(II) and zinc(II) complexes have been shown by Str. S1 to Str. S7. The results on antifungal and antibacterial activities of the new compounds have been included in Table S2 and Table S3 & Table S4, respectively. Supplementary Information is available at www.ias.ac.in/chemsci.

References

1. Hermann P, Kotek J, Kubíček V and Lukeš I 2008 Gadolinium(III) complexes as MRI contrast agents: ligand design and properties of the complexes *Dalton Trans*. **23** 3027
2. Bernhardt P V and Sharpe P C 2000 C-substituted macrocycles as candidates for radioimmunotherapy *Inorg. Chem.* **39** 4123
3. Biswas F B, Roy T G, Rahman M A and Emran T B 2014 An in vitro antibacterial and antifungal effects of cadmium(II) complexes of hexamethyltetraazacyclotetradecadiene ligands *Asian Pac. J. Trop. Biomed.* **7**(sup 1) 534
4. Roy T G, Hazari S K S, Dey B K, Miah H A, Olbrich F and Rehder D 2007 Syntheses and antimicrobial activities of isomers of N(4), N(11)-dimethyl-3,10-C-meso-3,5,7,7,10,12,14,14-octamethyl-1,4,8,11-tetraaza-cyclotetradecane and their nickel(II) complexes *Inorg. Chem.* **46** 5372
5. Parveez G and Athar A H 2015 Biological activity studies on metal complexes of macrocyclic Schiff base ligand: synthesis and spectroscopic characterization *J. Braz. Chem. Soc.* **26** 1331
6. Gull P, Dar O A, Malik M A and Hashmi A A 2016 Design, synthesis, characterization and antimicrobial/ antioxidant activities of 1, 4-dicarbonyl-phenyl dihydrazide based macrocyclic ligand and its Cu(II), Co(II) and Ni(II) complexes *Microb. Pathog.* **100** 237
7. EI-Boraey H A and EL-Gammal O A 2015 New 15-membered tetraaza (N4) macrocyclic ligand and its transition metal complexes: spectral, magnetic, thermal and anticancer activity *Spectrochim. Acta A* **138** 553
8. Rzuezek S G, Pilch D S, Liu A, Liu L, LaVoie E J and Rice J E 2010 Macrocyclic pyridyl polyoxazoles: selective RNA and DNA G-quadruplex ligands as antitumor agents *J. Med. Chem.* **53** 3632
9. Shankarwar S G, Nagolkar B B, Shelke V A and Chondhekar T K 2015 Synthesis, spectral, thermal and antimicrobial studies of transition metal complexes of 14-membered tetraaza[N4] macrocyclic ligand *Spectrochim. Acta A* **145** 188
10. Suh M P, Moon H R, Lee E Y and Jang S Y A 2006 Redox-active two-dimensional coordination polymer: preparation of silver and gold nanoparticles and crystal dynamics on guest removal *J. Am. Chem. Soc.* **128** 4710
11. Singh A K, Panwar A, Kumar S and Baniwal S 1999 Chromium(III)-selective electrode based on a macrocyclic compound *Analyst* **124** 521
12. Roy T G, Hazari S K S, Meah H A, Gupta S K D, Roy P G, Behrens U and Rehder D 2014 Synthesis and antimicrobial activities of copper(II) complexes of N(4),N(11)-dimethyl (L_{BZ} & L_{CZ}) and N(4)-monomethyl(L_{CZ1})(-3,5,7,7,10,12,14,14-octamethyl-1,4,8,11-tetraazacyclotetradecane. Crystal and molecular structure of $[CuL_{CZ1}](ClO_4)_2$ *Inorg. Chim. Acta* **415** 124
13. Roy T G, Hazari S K S, Dey B K, Meah H A, Bader C and Rehder D 2004 Copper(II) and nickel(II) complexes of N,N-bis(2-hydroxyethyl)-octamethyl-1,4,8,11-tetraaza-cyclotetradecane *Eur. J. Inorg. Chem.* **2004** 4115
14. Rabi S, Mia H A, Hazari S K S, Roy T G and Manchur M A 2018 Nickel(II) complexes with N-pendent macrocyclic ligands: synthesis, characterization and antimicrobial activities *Int. J. Int. Sci. Technol.* **3** 75
15. Alam, M S, Rabi S, Rahman M M, Baidya A, Debi M and Roy T G 2018 Synthesis, characterization and antimicrobial studies of cadmium(II) complexes with a tetraazamacrocycle (L_B) and its cyanoethyl N-pendent derivative (L_{BX}) *J. Chem. Sci.* **130** 1
16. Roy T G, Hazari S K S, Dey B K, Miah H A and Tiekink E R T 2001 Trans-(3S,5S,10R,12R)-1,8-bis(2-cyanoethyl)-C-meso-3,5,7,7,10,12,14,14-octamethyl-1,4,8,11-tetraazacyclotetradecane *Acta Cryst.* **E57** 0524
17. Roy T G, Hazari, S K S, Dey B K, Chakraborty S and Tiekink E R T 1999 Synthesis, characterization and antifungal activities of some new copper(II) complexes of octamethyl tetraazacyclotetradecadiene *Met. Based Drugs* **6** 345
18. Bembi R, Roy T G, Jhanji A K and Mahewari 1990 A Polyazamacrocycles. Part 7 Kinetics of aquation of trans-dichloro and *trans*-chloro(nitro) complexes of cobalt(III) with tera-aza macrocycles *J. Chem. Soc. Dalton Trans.* **11** 3531
19. Roy T G, Bembi R, Hazari S K S, Dey B K, Acharjee T K, Horn E and Tiekink E R T 2002 Characterization of diastereoisomeric $[Ni(Me_8[14]ane)]^{2+}$ cations *J. Coord. Chem.* **55** 853
20. Roy T G, Hazari S K S, Dey B K, Meah H A, Rahman M S, Kim D I and Park Y C 2007 Synthesis, electrolytic behavior and antimicrobial activities of cadmium complexes of isomers of 3,10-C-meso-3,5,7,7,10,12,14,14-octamethyl-1,4,8,11-tetraazacyclotetradecane *J. Coord. Chem.* **40** 1567
21. Curtis N F, Swann S A, Waters T N and Maxwell I E 1969 Isomerism of some octamethyl-1,5,8,12-tetraaza-cyclotetradecadiene complexes of nickel(II) and copper(II) *J. Am. Chem. Soc.* **91** 4588
22. Nakamoto K 1963 *Infrared Spectra of Inorganic and Coordination Compounds* Second edn. (New York: John Wiley & Sons) p. 187
23. Bembi R, Drew M G B, Singh R and Roy T G 1991 Polyazamacrocycles. 9. Characterisation of diastereoisomeric trans-$(Co(Me_8[14]ane)Cl_2]^+$ complexes *Inorg. Chem.* **30** 1403

24. Roy T G, Bembi R., Hazari S K S, Dey B K, Acharjee T K, Horn E and Tiekink E R T 2002 Characterization of diastereoisomeric [Ni(Me$_8$[14]ane)]$^{2+}$ cations *J. Coord. Chem.* **55** 853

25. Farago M E and James J M 1965 Coordination of thiocyanate and selenocyanate in some diamine complexes of nickel(II) and copper(II) *Inorg. Chem.* **4** 1706

26. Sabatini A and Bertin I 1965 Infrared Spectra between 100 and 2500 cm^{-1} of some complex metal cyanates, thiocyanates and selenocyanates *Inorg. Chem.* **4** 959

27. Conley R T 1966 *Infrared Spectroscopy* (Boston, Massachusetts: Allyn and Bacon)

28. Geary W J 1971 The use of conductivity measurements in organic solvents for the characterization of coordination compounds *Coord. Chem. Rev.* **7** 81

29. Bembi R, Bhardwaj V K, Singh R, Teneja K and Aftab S 1984 Synthesis and characterization of copper(II), nickel(II) and cobalt(III) complexes with 1,4,8,11-tetraazacyclohexadecane and 1,4,8,11-tetraazacyclo pheptadecane *Inorg. Chem.* **23** 4153

30. Martrin L Y, Sperati C R and Busch D H 1977 The spectrochemical properties of tetragonal complexes of high spin nickel(II) containing macrocyclic ligands *J. Chem. Soc.* **99** 2968

31. Roy T G, Hazari S K S, Dey B K, Chakraborty S and Tiekink E R T 1999 Synthesis, characterisation and antifungal activities of some new copper(II) complexes of octamethyl tetraazacyclotetradecadiene *Met. Based Drugs* **6** 345

32. Mochizuki K and Kondo 1995 Isolation and Vis-Absorption Spectrum of trans [Ni(OH$_2$)$_2$(cyclam)]Cl$_2$.cntdot.4H$_2$OT *Inorg. Chem.* **34** 6241

33. Chandra S and Krishan S K 1983 Synthesis and characterization of copper(II) complexes of a macrocyclic Ligand *Trans. Met. Chem.* **8** 1

34. Chandra S, Tyagi M and Agrawal S 2010 Synthesis and characterization of a tetraaza macrocyclic ligand and its cobalt(II), nickel(II) and copper(II) complexes *J. Serb. Chem. Soc.* **75** 935

35. Jorgensen J H and Ferrar M J 2009 Antimicrobial susceptibility testing: a review of general principles and contemporary practices *Clin. Infect. Dis.* **49** 1749

36. Salehi M and Hasanzadeh M 2015 Characterization, crystal structures, electrochemical and antibacterial studies of four new binuclear cobalt(III) complexes derived from o-aminobenzyl alcohol *Inorg. Chim. Acta* **426** 6

37. Dharmaraj N, Viswanathamurthi P and Nataranjan K 2001 Ruthenium(II) complexes containing bidentate Schiff bases and their antifungal activity *Trans. Met. Chem.* **26** 105